ARTICLE

Time-Resolved Single-Step Protease Activity Quantification Using Nanoplasmonic Resonator Sensors

Cheng Sun,[†,⊥,*] Kai-Hung Su,[†] Jason Valentine,[†] Yazmin T. Rosa-Bauza,[‡] Jonathan A. Ellman,[‡] Omeed Elboudwarej,[§] Bipasha Mukherjee,[§] Charles S. Craik,[∥] Marc A. Shuman,[∥] Fanqing Frank Chen,[§,∥,*] and Xiang Zhang[†,*]

[†]Nanoscale Science and Engineering Center (NSEC), 5130 Etcheverry Hall, University of California, Berkeley, California 94720, Department of Mechanical Engineering, Northwestern University, Evanston, Illinois 60208-3111, [‡]Department of Chemistry, University of California, Berkeley, California 94720, [§]Lawrence Berkeley National Laboratory, Berkeley, California 94720, and [∥]Comprehensive Cancer Center, University of California, San Francisco, California 94143. [⊥]Present address: Department of Mechanical Engineering, Northwestern University, Evanston, Illinois 60208-3111.

ABSTRACT Protease activity measurement has broad application in drug screening, diagnosis and disease staging, and molecular profiling. However, conventional immunopeptidemetric assays (IMPA) exhibit low fluorescence signal-to-noise ratios, preventing reliable measurements at lower concentrations in the clinically important picomolar to nanomolar range. Here, we demonstrated a highly sensitive measurement of protease activity using a nanoplasmonic resonator (NPR). NPRs enhance Raman signals by 6.1×10^{10} times in a highly reproducible manner, enabling fast detection of proteolytically active prostate-specific antigen (paPSA) activities in real-time, at a sensitivity level of 6 pM (0.2 ng/mL) with a dynamic range of 3 orders of magnitude. Experiments on extracellular fluid (ECF) from the paPSA-positive cells demonstrate specific detection in a complex biofluid background. This method offers a fast, sensitive, accurate, and one-step approach to detect the proteases' activities in very small sample volumes.

KEYWORDS: plasmonic resonator · surface-enhanced Raman scattering · sensing · prostate cancer · protease

*Address correspondence to xiang@berkeley.edu, c-sun@northwestern.edu, f_chen@lbl.gov.

Received for review July 7, 2009 and accepted January 25, 2010.

Published online February 2, 2010. 10.1021/nn900757p

Originally developed in 1928, Raman spectroscopy has been used extensively to characterize molecular properties.[1] Surface-enhanced Raman spectroscopy (SERS) increases the Raman signal significantly[2−5] through enhanced electromagnetic fields in close proximity to a surface. Additional enhancement can be obtained by utilizing molecular resonance Raman (RR) effect when the molecule was excited at its absorption band.[6] SERS measurements performed on dispersed metal nanoparticle aggregates, which is the most commonly used SERS substrate,[7] have demonstrated detection sensitivity up to single molecule level.[8−10] However, these measurements often suffer from poor reproducibility.[11] To improve the reproducibility, other methods, including self-assembly of metallic colloidal nanoparticles,[12] nanosphere lithography (NSL) and metal film over nanosphere (MFON),[13] electrochemical roughening of polished gold substrate,[14] and periodic structured metallic substrate using electron-beam lithography,[15] have been developed to fabricate a SERS substrate consisting of homogeneous features over a large area with reproducible enhancement factors up to 10^8. Although these efforts lead to successful utilization of SERS analysis in many promising applications, including gene and protein discrimination,[16−18] biowarfare agent detection,[19] and real-time glucose monitoring,[20] the inability to fabricate SERS hot-spots at a specific location limits application for a very small sample volume. To overcome such a limit, we recently developed tunable nanoplasmonic resonators (NPRs), consisting of a thin SiO_2 layer sandwiched between metallic nanodisks.[21] The resonance frequency can be precisely tuned by varying the dielectric layer thickness and aspect ratio of the NPRs. Individual NPRs can enhance the Raman intensity by a factor of 6.1×10^{10}, among the largest values obtained for a single SERS substrate or nanoparticle. Fabricated using well-established nanolithography processes, the NPR-based method enables producing SERS hot-spots at a desired location in a much smaller dimension reproducibly, allowing multiplexed high-throughput detection and lab-on-chip applications.

Prostate cancer biomarker, prostate-specific antigen (PSA), a kallikrein (hK) family serine protease,[22,23] is used as the model protease in this study. The commonly used PSA blood test has been widely used for early diagnosis and management of prostate cancer, the leading

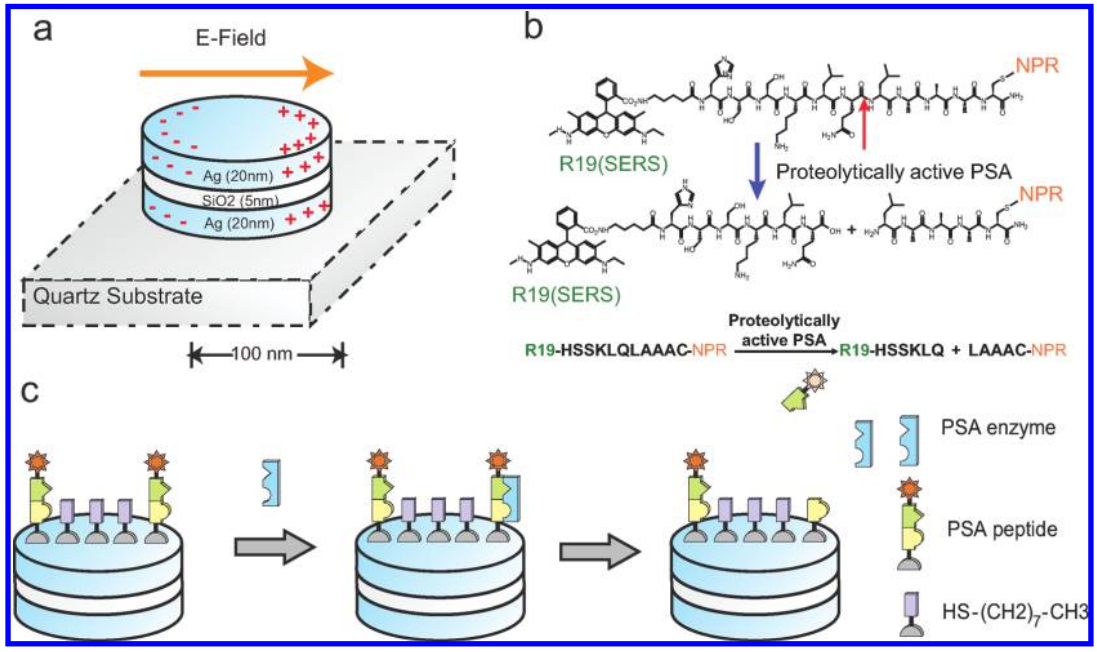

Figure 1. Schematic illustration of the working principle of detecting PSA protease activity using peptide-conjugated NPR SERS nanosensors. (a) NPRs exhibit a tunable plasmon resonance and highly enhanced local electromagnetic field through coupled plasmonic resonance. NPRs with a short axis of 150 nm and a long axis of 200 nm were made of multistacks of silver and SiO_2 layers with thicknesses of 25 and 5 nm, respectively. (b) Molecular structure of the biomarker that consists of Raman dye R19, PSA specific peptide sequence HSSKLQLAAAC, and cysteine. The peptide can be cleaved by PSA enzyme between HSSKLQ and LAAAC. (c) Detection scheme of NPR functionalized with peptide sequence HSSKLQLAAAC and the Raman dye R19 (star). The presence of the PSA enzyme will cleave the peptide sequence. After cleavage, the diffusion of the R19 (star) away from the surface will be monitored by the loss of the SERS signatures of the R19 moiety. Packing molecule octanethiol ($HS-(CH_2)_2-CH_3$) was used to reduce the packing density of the reporting peptide on the NPR surface and, thus, allows the PSA enzyme to access the reporting peptide.

male cancer.[24,25] However, serum PSA concentrations reflect the presence of benign prostatic hyperplasia (BPH) more often than cancer.[26,27] The lack of specificity causes a high false-positive rate and often leads to costly prostate needle biopsies for diagnosis and postbiopsy complications as well as considerable anxiety.[22,28,29] Recent research has identified a family of highly specific peptides that can be cleaved by paPSA isoform in xenograft models[30] and human samples;[31,32] thus, measurement of paPSA protease activity from *in vivo* samples is possible and would be potentially valuable as a more specific screening agent for prostate cancer and in detection of recurrent disease. However, reported results based on immunopeptidemetric assays (IMPA) exhibit low fluorescence signal-to-noise ratios, preventing reliable measurements at lower concentrations in the clinically important range of 60−300 pM.[31,32] In addition, there is usually a limited number of prostate cancer cells (<1000) isolated from fine needle biopsy or circulating cell capture. No method exists that can perform a paPSA protease activity assay on a small number of cells for clinical staging. Therefore, a key goal of this work is to develop an NPR-based method that allows specific and sensitive measurements of paPSA for prostate cancer detection in a very small sample volume.

RESULTS AND DISCUSSION

In this work, NPRs (Figure 1a) were conjugated with a PSA protease-specific substrate peptide, which has the sequence R19-HSSKLQLAAAC,[30,33] with the SERS molecule Rhodamine 19 (R19) at the N-terminus and cysteine at the C-terminus (Figure 1b). The peptide has been identified as a highly specific peptide that can be cleaved by paPSA *in vivo* in xenograft models[30] and human samples.[31,32] The paPSA cleaves the peptide, leading to the release of the R19 moiety (Figure 1c) and a subsequent decrease in the Raman scattering intensity in a dose- and time-dependent manner, and the PSA protease activity can be accurately quantified. It has been theoretically estimated that SERS enhancement is strongly localized to the vicinity of nanoparticle resonator surface (5−10 nm), which effectively eliminates the assay background noise from the Raman scattering substance in the surrounding fluids or the R19 moieties that diffuse into the solution after protease cleavage. Because of this unique property, the assay can be performed in a simplified one-step format with no additional washing step required.

Under an optical microscope, the NPR arrays were distinctly visible due to the strong scattering of light at their resonant wavelength (Figure 2a). The magnified views of NPR arrays measured by scanning electron microscopy (SEM) and atomic force microscopy

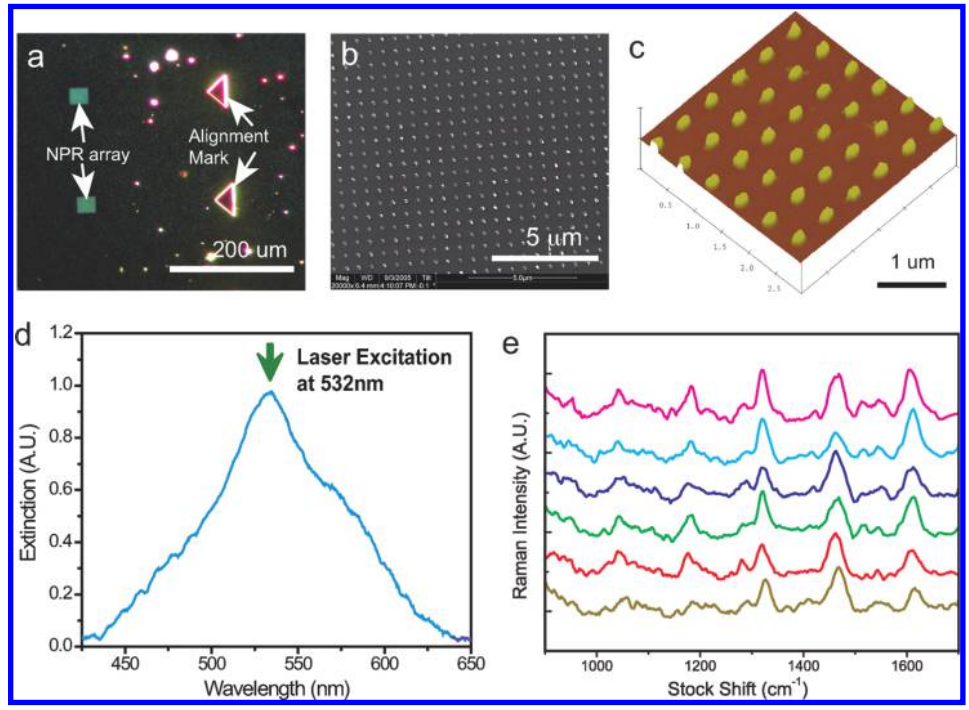

Figure 2. (a) Optical microscopic image of NPR arrays fabricated using standard e-beam lithography and a thin film deposition process. Fabricated NPR arrays consist of 30 × 30 NPRs with 500 nm spacing. Multiple NPR arrays and an alignment mark can be conveniently fabricated on the same substrate. (b) Magnified image of an NPR array measured by SEM. Using precision lithography methods, the NPR can be prepared in a controlled manner. (c) NPRs measured at higher magnification using AFM. (d) Measured extinction spectrum of an NPR−peptide−R19 conjugate array at a wavelength range of 425 to 650 nm. The resonance peak of the NPR has been tuned to closely match the laser excitation and Raman emission frequencies and, thus, maximizes the overall enhancement of the Raman signal. (e) Reproducible Raman spectra of NPR−peptide−R19 conjugates measured from six different NPR arrays. Integration time is 30 s.

(AFM) are shown in Figure 2b,c. The optical properties of the NPR were characterized by illuminating the NPRs with collimated light delivered by a multimode optical fiber from a 150 W xenon lamp (Thermo Oriel), and the extinction spectra were collected using a grating spectrometer (Triax 550, Jobin Yvon) with a matched liquid nitrogen cooled CCD detector (CCD-3500, Jobin Yvon).[21] The SiO_2 layer, sandwiched between the Ag layers, enabled precisely tuning of the NPR resonance. As shown in Figure 2d, the measured resonance peak of NPR−peptide−R19 conjugates closely matches the laser excitation wavelength at 532 nm and, thus, maximizes the enhancement of Raman scattering. It is worthwhile to note, at the laser excitation overlap with the R19 absorption band centered at 517 nm, the resulting resonant Raman scattering may also contribute to the enhanced Raman signal. For the SERS experiments, Raman spectra were measured using a modified inverted microscope (Axiovert 200, Zeiss) with a 50× objective in a backscattering configuration. As shown in Figure 2e, the NPR-based SERS substrate exhibits a reproducible Raman spectrum with consistent enhancement factor at the same order of magnitude. The variation of experimentally measured SERS intensities obtained from six different NPR arrays is below 25%, and it can be easily normalized in the experiment.

The assay was performed by exposing the NPR−peptide−R19 nanosensor to the fluidic samples, and the subsequent time-dependent R19 Raman spectra change was recorded at an interval of 1 min and an integration time of 30 s. The Raman peak at 1316 cm^{-1} of SERS label molecule (R19) was monitored as the primary signature peak in this study, while the 1456, 1526, and 1597 cm^{-1} peaks were also monitored as additional references (Figure 3). The time-resolved spectral measurement in the presence of PSA (Figure 3a) is plotted in Figure 3c. Because the SERS intensities are proportional to the remaining R19 on the NPR surface, the normalized SERS intensity change is a direct indicator of PSA activity. Despite the variation in the initial intensity of different Raman signature peaks, the normalized data all converged into the same curve, indicating that the normalized SERS intensity change is a reliable measure to quantitatively determine the substrate peptide being cleaved. As shown in Figure 3c, before PSA addition, the NPR nanosensor showed steady intensities for all of the peaks over a 10 min period. However, upon addition of PSA, a significant decrease in each Raman peak is observed in the first 10−12 min, indicating that the PSA pro-

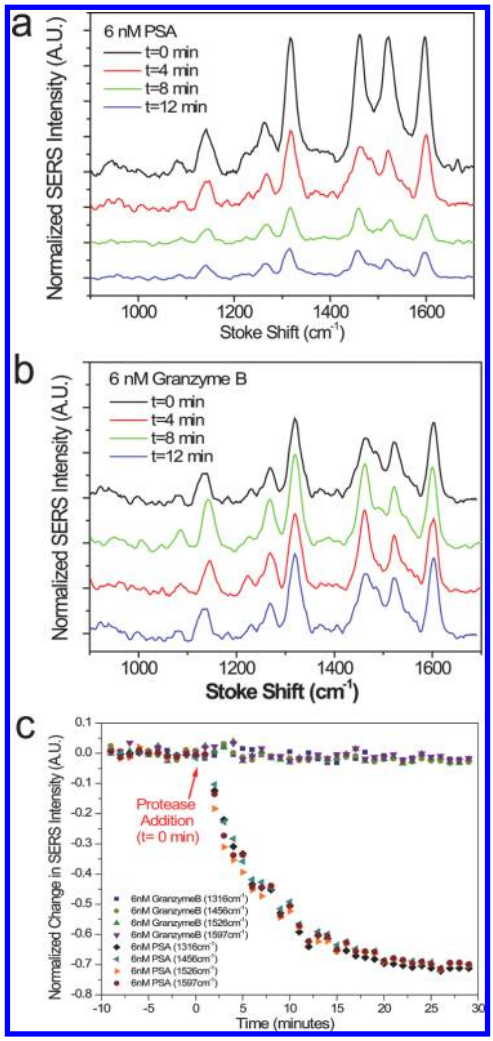

Figure 3. Real-time kinetic measurement of PSA protease activity. (a) SERS spectra for 6 nM PSA incubation taken over 30 min with an integration time of 30 s. (b) SERS spectra for the negative control, 6 nM granzyme B, taken over 30 min. (c) Time-resolved measurements of relative change in Raman peak intensity at 1316, 1456, 1526, and 1597 cm^{-1} before and after addition of PSA protease. Negative time represents time before protease addition.

tease was able to cleave the peptides on the NPR. At the end point of 30 min, the decrease of the Raman signal reaches a plateau at a PSA concentration of 6 nM, while at a lower concentration level (~pM), the signal continues to decrease at a much lower rate. Another serine protease, granzyme B, was selected as a negative control (Figure 3b,c). Within 50 min of recording, no substantial changes in SERS intensity were observed, even at concentrations up to 1 μM. This result demonstrates that the decrease of Raman signal in the PSA assay was based on a genuine enzymatic process, rather than a nonspecific hydrolysis reaction or due to the displacement of the peptide from the surface by other components in the buffer.

The sensitivity of the NPR nanosensor was evaluated by measuring the SERS intensity change of a set of samples with the PSA enzyme concentration ranging from 6 nM to 6 pM. The absolute value of normalized SERS intensity change is shown in Figure 4a. As expected, the rate of decrease in the Raman signal was proportional to the concentration of PSA, which is explained by a reduced rate of peptide cleavage when the PSA concentrations are decreased. The proteolytic activity eventually reaches an equilibrium stage at 30 min, as indicated by each Raman signal reaching a plateau. The absolute value of normalized decrease in SERS intensity *versus* various concentrations, after 30 min of enzyme addition, is plotted in Figure 4b. The dynamic range for detection, in the current assay setup, was from 6 pM to 6 nM. PSA concentration higher than 6 nM does not exhibit a distinct difference with the given detection time. As shown in Figure 4c, the monitored Raman peak intensity exhibits distinguishable decay characteristics at different PSA concentrations during the initial 4 min of sampling. Thus, by fitting the decaying rate, reliable assays can possibly be accomplished in 4 min.

In addition to protease activity measurements of purified PSA, measurements for PSA protease activity in extracellular fluid (ECF) from live cell culture were performed (Figure 4d). It is well-known that LNCaP cells secrete PSA and have recently been used in xenografts to evaluate *in vivo* PSA concentration.[30] For comparison, a K562 cell line, which does not secrete PSA into the ECF, was used as a negative control. LNCaP ECF showed a significant change in SERS signal, while K562 exhibits very low PSA enzymatic activity (Figure 4d). By correlating the normalized decrease in Raman signal with Figure 3b, it was determined that the LNCaP media had an elevated amount of paPSA concentration (Figure 4d).

SUMMARY

Compared with fluorescence-based assay, the NPR-based method offers several advantages. Strongly localized Raman enhancement can substantially amplify the signal and also effectively reduce background noise. Therefore, it allows one-step and label-free detection of protease activity with sensitivity at 6 pM and a dynamic range of 3 orders of magnitude. It should be noted that PSA is considered a weak protease, and other proteases would allow even better sensitivity. Second, it allows accurate measurement with a very small sample volume of 15 pL (Supporting Information). Third, fabricated using a well-established nanolithography process, the NPR-based method is highly reproducible and thus allows quantitative assessment of protease activity. Finally, NPRs can be spatially arranged in a microarray format to achieve multiplexed measurements with broad applications, by measuring all known proteases in unprocessed biological samples without complex sample processing and purification steps. The multiplexity of the substrate peptide spatially

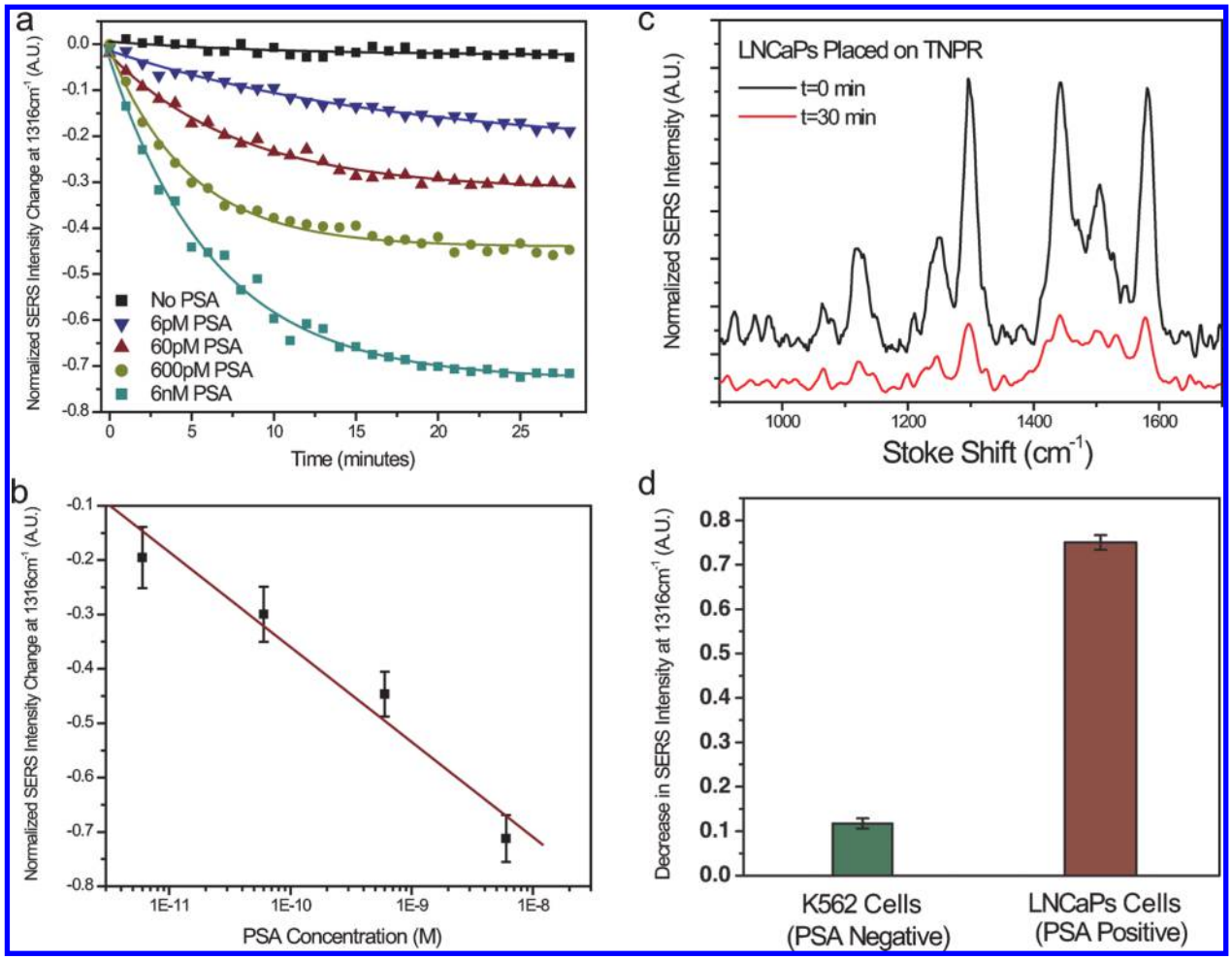

Figure 4. Time-resolved measurements of PSA activity by varying the active PSA concentration. (a) Normalized SERS intensity change for 1316 cm^{-1} peak at active PSA concentration from 6 pM to 6 nM. The decreasing of SERS intensity can be clearly measured, while no significant change can be observed in the control experiment with no active PSA protease. (b) Concentration dependence of normalized SERS intensity change obtained at 30 min. (c) Protease activity measurement obtained from unprocessed extracellular fluid (ECF): Raman spectra obtained at the beginning of exposing LNCaP cells (positive control) ECF to NPR nanosensors (t = 0 min) and after 30 min. (d) Normalized change of SERS intensity at 1316 cm^{-1} peak indicating PSA proteolytic activity in the fluid extracted from LNCaP and K562 cell lines.

can be achieved with a microarrayer with industry standard protocols when combined with NPR nanoarray clusters arranged in the microarray format. Even if each of the 500+ proteases are cross-interrogated by 10 different substrate peptides, the array still has an easily manageable feature number of less than 10 000.[34]

MATERIALS AND METHODS

NPR Fabrication. The NPR was patterned on quartz substrates (HOYA Corp.) by electron beam lithography (EBL) (Nanowriter Series EBL 100, Leica Microsystems). A 30 nm thick indium−tin−oxide (ITO) under-layer was sputtered on the substrate to prevent charging effects during the EBL process. A 100 nm thick polymethylmethacrylate (PMMA, MicroChem Corp.) film spin-coated on the ITO-quartz glass was used as a positive photoresist. After exposure, the patterns were developed using a 1:3 ratio of a MIBK and IPA mixture followed by multilayer deposition of metal and dielectric materials using electron beam evaporation (Mark 40, CHA) and standard lift-off procedures. We fabricated three layered Ag/SiO_2/Ag NPR arrays with each silver and SiO_2 layer thickness equal to 25 and 5 nm, respectively. The geometry of the fabricated NPR was examined by atomic force microscopy, and the total thickness of the NPR is confirmed to be 55 nm.

Device Design and Characterization. The optical properties of the NPR were characterized by illuminating the NPRs with collimated light delivered by a multimode optical fiber from a 150 W xenon lamp (Thermo Oriel) and collecting the extinction spectra using a grating spectrometer (Triax 550, Jobin Yvon) with a matched liquid nitrogen cooled CCD detector (CCD-3500, Jobin Yvon). For the SERS experiments, Raman spectra were measured using a modified inverted microscope (Axiovert 200, Zeiss) with a 50× objective in a backscattering configuration. Baseline subtraction was applied to remove the fluorescence background of the measured spectra. The spectra were then smoothed in Matlab using the Savitsky−Golay method with a second-order polynomial and window size of 9. To correct the possible influence due to the fluctuation of illumination intensity, frequency dependence of Raman scattering, and the variation of initial packing density of the reported molecules, the change in SERS intensity was normalized to the average intensity before protease addition. The normalized SERS intensity change is defined as

$$\Delta I = [I_t - I_0]/I_0$$

where I_0 is the average SERS intensity before the addition of the protease and I_t is the SERS intensity measured at the given time t.

Peptide Conjugation to NPR and Applying Sample. The peptide attaches to the NPR *via* the thiol group on cysteine. The PSA substrate peptides were mixed with octanethiol at a 1:3 ratio and at a concentration of 50 μM. Octanethiol, with a SAM chain length of 1−2 nm, was used as packing material to manage the distance among the PSA substrate peptides and help to erect the PSA substrate peptide for optimal spatial presentation. Thus, the octanethiol SAM improves access for the protease to bind to the peptides. The peptide solution was incubated with the NPR substrate for 24 h to ensure a well-ordered self-assembled monolayer on the NPR metallic surface. During incubation, the sample was kept at 20 °C. Before incubation with the PSA enzyme, the sample was washed repeatedly with deionized water to ensure that all of the unattached peptides were removed. Upon washing, the sample was incubated with a sample in a Tris-HCl, pH 8.0, 100 mM NaCl, and 0.1 mM EDTA buffer. Incubation was performed by placing a 100 μL drop of the sample on the NPR array. SERS measurements were performed directly after incubation at 1 min intervals.

Cell Culture and Clinical Semen Samples. LNCaP cells actively secrete PSA into ECF, and the human CML cells K562 are negative for PSA. Both cell lines are maintained in RPMI-1640 with 10% FBS and 1× Pen/Strep, at 37 °C with 5% CO_2; 10×10^6 cells were cultured overnight in 10 mL of fresh media. Media from both cultures were collected, and PSA activity was measured by fluorescent methods as described before and calibrated against commercial PSA (Calbiochem, San Diego, CA). Briefly, the PSA-binding peptides and derivatives with a spacer were chemically synthesized and used to prepare an affinity column, which was used to fractionate PSA in seminal plasma.

Purified PSA Preparation and Proteolytic Reaction. Proteolytically active PSA was purified to homogeneity from human seminal plasma by column chromatography, eliminating all known PSA complexes and retaining its protease fraction. Cleavage of the substrate peptide immobilized on the NPR nanosensor is performed in a buffer of 50 mM Tris-HCl, pH 8.0, 100 mM NaCl, and 0.1 mM EDTA, and the reaction was monitored in real-time in 37 °C. Protease inhibitors (to prevent PSA and granzyme B degradation) were obtained from CalBiochem and added to the reaction mixture following the manufacturer's instructions, so that the final reaction solution contains 5 μM AEBSF, 4.2 nM Aprotinin, 200 nM Elastatinal, and 10 nM GGACK. The concentration of proteolytically active PSA in the PSA reagent has been prepared with a wide range of concentration from 6 pM to 6 nM.

Acknowledgment. We thank Dr. R. Oulton for useful discussion and help with the manuscript. This work is supported by National Institutes of Health (NIH) through NIH Roadmap for Medical Research (PN2EY018228), National Science Foundation (NSF) Nanoscale Science and Engineering Center (CMMI-0751621), and NSFSST/Collaborative Research Program (DMI-0427679). F.C. is supported by NHLBI/NIH HL078534 and NCI/NIH R1CA95393-01, DARPA, and UCSF Prostate Cancer SPORE award (NIH Grant P50 CA89520). J.A.E. and Y.T.R.-B. were supported by P01 CA072006. This work was performed under the auspices of the U.S. Department of Energy, at the University of California/Lawrence Berkeley National Laboratory, under Contract No. DE-AC03-76SF00098.

Supporting Information Available: Peptide synthesis, instrumentation setup, and estimation of the detection volume. This material is available free of charge *via* the Internet at http://pubs.acs.org.

REFERENCES AND NOTES

1. Ferraro, J. R.; Nakamoto, K.; Brown C. W. *Introductory Raman Spectroscopy*, 2nd ed.; Elsevier Science: Amsterdam, 2003; p 434.
2. Yonzon, C. R.; Haynes, C. L.; Zhang, X.; Walsh, J. T., Jr.; Van Duyne, R. P. A Glucose Biosensor Based on Surface-Enhanced Raman Scattering: Improved Partition Layer, Temporal Stability, Reversibility, and Resistance to Serum Protein Interference. *Anal. Chem.* **2004**, *76*, 78–85.
3. Grow, A. E.; Wood, L. L.; Claycomb, J. L.; Thompson, P. A. New Biochip Technology for Label-Free Detection of Pathogens and Their Toxins. *J. Microbiol. Methods* **2003**, *53*, 221–233.
4. Nithipatikom, K.; McCoy, M. J.; Hawi, S. R.; Nakamoto, K.; Adar, F.; Campbell, W. B. Characterization and Application of Raman Labels for Confocal Raman Microspectroscopic Detection of Cellular Proteins in Single Cells. *Anal. Biochem.* **2003**, *322*, 198–207.
5. Jackson, J. B.; Halas, N. J. Surface-Enhanced Raman Scattering on Tunable Plasmonic Nanoparticle Substrates. *Proc. Natl. Acad. Sci. U.S.A.* **2004**, *101*, 17930–17935.
6. Hildebrandt, P.; Stockburger, M. Surface-Enhanced Resonance Raman-Spectroscopy of Rhodamine-6g Adsorbed on Colloidal Silver. *J. Phys. Chem.* **1984**, *88*, 5935–5944.
7. Stiles, P. L.; Dieringer, J. A.; Shah, N. C.; Van Duyne, R. R. Surface-Enhanced Raman Spectroscopy. *Annu. Rev. Anal. Chem.* **2008**, *1*, 601–626.
8. Kneipp, K.; Kneipp, H.; Itzkan, I.; Dasari, R. R.; Feld, M. S. Surface-Enhanced Raman Scattering: A New Tool for Biomedical Spectroscopy. *Curr. Sci.* **1999**, *77*, 915–924.
9. Nie, S.; Emory, S. R. Probing Single Molecules and Single Nanoparticles by Surface-Enhanced Raman Scattering. *Science* **1997**, *275*, 1102–1106.
10. Le Ru, E. C.; Blackie, E.; Meyer, M.; Etchegoin, P. G. Surface Enhanced Raman Scattering Enhancement Factors: A Comprehensive Study. *J. Phys. Chem. C* **2007**, *111*, 13794–13803.
11. Moskovits, M. Surface-Enhanced Spectroscopy. *Rev. Mod. Phys.* **1985**, *57*, 783–826.
12. Freeman, R. G.; Grabar, K. C.; Allison, K. J.; Bright, R. M.; Davis, J. A.; Guthrie, A. P.; Hommer, M. B.; Jackson, M. A.; Smith, P. C.; Walter, D. G.; Natan, M. J. Self-Assembled Metal Colloid Monolayers—An Approach to SERS Substrates. *Science* **1995**, *267*, 1629–1632.
13. Haynes, C. L.; Van Duyne, R. P. Plasmon-Sampled Surface-Enhanced Raman Excitation Spectroscopy. *J. Phys. Chem. B* **2003**, *107*, 7426–7433.
14. Sylvia, J. M.; Janni, J. A.; Klein, J. D.; Spencer, K. M. Surface-Enhanced Raman Detection of 1,4-Dinitrotoluene Impurity Vapor as a Marker To Locate Landmines. *Anal. Chem.* **2000**, *72*, 5834–5840.
15. Kahl, M.; Voges, E.; Kostrewa, S.; Viets, C.; Hill, W. Periodically Structured Metallic Substrates for SERS. *Sens Actuators, B* **1998**, *51*, 285–291.
16. Cao, Y. C.; Jin, R. C.; Nam, J. M.; Thaxton, C. S.; Mirkin, C. A. Raman Dye-Labeled Nanoparticle Probes for Proteins. *J. Am. Chem. Soc.* **2003**, *125*, 14676–14677.
17. Cao, Y. W. C.; Jin, R. C.; Mirkin, C. A. Nanoparticles with Raman Spectroscopic Fingerprints for DNA and RNA Detection. *Science* **2002**, *297*, 1536–1540.
18. Vo-Dinh, T.; Yan, F.; Wabuyele, M. B. Surface-Enhanced Raman Scattering for Medical Diagnostics and Biological Imaging. *J. Raman Spectrosc.* **2005**, *36*, 640–647.
19. Stuart, D. A.; Biggs, K. B.; Van Duyne, R. P. Surface-Enhanced Raman Spectroscopy of Half-Mustard Agent. *Analyst* **2006**, *131*, 568–572.
20. Lyandres, O.; Shah, N. C.; Yonzon, C. R.; Walsh, J. T.; Glucksberg, M. R.; Van Duyne, R. P. Real-Time Glucose Sensing by Surface-Enhanced Raman Spectroscopy in Bovine Plasma Facilitated by a Mixed Decanethiol/Mercaptohexanol Partition Layer. *Anal. Chem.* **2005**, *77*, 6134–6139.
21. Su, K, D. S.; Steel, M. J.; Xiong, Y; Sun, C.; Zhang, X. Raman Enhancement Factor of Single Tunable Nano-Plasmonic Resonator. *J. Phys. Chem. B* **2006**, *110*, 3964–3968.
22. Denmeade, S. R.; Isaacs, J. T. The Role of Prostate-Specific Antigen in the Clinical Evaluation of Prostatic Disease. *BJU Int.* **2004**, *93*, 10-5.
23. Clements, J. A.; Willemsen, N. M.; Myers, S. A.; Dong, Y. The Tissue Kallikrein Family of Serine Proteases: Functional Roles in Human Disease and Potential as Clinical Biomarkers. *Crit. Rev. Clin. Lab Sci.* **2004**, *41*, 265–312.

24. Gronberg, H. Prostate Cancer Epidemiology. *Lancet* **2003**, *361*, 859–864.
25. Denmeade, S. R.; Isaacs, J. T. A History of Prostate Cancer Treatment. *Nat. Rev. Cancer* **2002**, *2*, 389–396.
26. Caplan, A.; Kratz, A. Prostate-Specific Antigen and the Early Diagnosis of Prostate Cancer. *Am. J. Clin. Pathol.* **2002**, *117*, S104-8.
27. Canto, E. I.; Shariat, S. F.; Slawin, K. M. Molecular Diagnosis of Prostate Cancer. *Curr. Urol. Rep.* **2004**, *5*, 203–211.
28. Gretzer, M. B.; Partin, A. W. PSA Markers in Prostate Cancer Detection. *Urol. Clin. North Am.* **2003**, *30*, 677–686.
29. Haese, A.; Graefen, M.; Huland, H.; Lilja, H. Prostate-Specific Antigen and Related Isoforms in the Diagnosis and Management of Prostate Cancer. *Curr. Urol. Rep.* **2004**, *5*, 231–240.
30. Denmeade, S. R.; Jakobsen, C. M.; Janssen, S.; Khan, S. R.; Garrett, E. S.; Lilja, H.; Christensen, S. B.; Isaacs, J. T. Prostate-Specific Antigen-Activated Thapsigargin Prodrug as Targeted Therapy for Prostate Cancer. *J. Natl. Cancer Inst.* **2003**, *95*, 990–1000.
31. Wu, P.; Stenman, U. H.; Pakkala, M.; Narvanen, A.; Leinonen, J. Separation of Enzymatically Active and Inactive Prostate-Specific Antigen (PSA) by Peptide Affinity Chromatography. *Prostate* **2004**, *58*, 345–353.
32. Wu, P.; Zhu, L.; Stenman, U. H.; Leinonen, J. Immunopeptidometric Assay for Enzymatically Active Prostate-Specific Antigen. *Clin. Chem.* **2004**, *50*, 125–129.
33. Denmeade, S. R.; Lou, W.; Lovgren, J.; Malm, J.; Lilja, H.; Isaacs, J. T. Specific and Efficient Peptide Substrates for Assaying the Proteolytic Activity of Prostate-Specific Antigen. *Cancer Res.* **1997**, *57*, 4924–4930.
34. Vo-Dinh, T.; Stokes, D. L.; Griffin, G. D.; Volkan, M.; Kim, U. J.; Simon, M. I. Surface-Enhanced Raman Scattering (SERS) Method and Instrumentation for Genomics and Biomedical Analysis. *J. Raman Spectrosc.* **1999**, *30*, 785–793.